

# Monitoring singlet oxygen *in situ* with delayed chemiluminescence to deduce the effect of photodynamic therapy

Yanchun Wei  
Da Xing  
Shiming Luo  
Wei Xu

South China Normal University  
Ministry of Education Key Laboratory of Laser  
Life Science  
Guangzhou 510631 China

Qun Chen

South China Normal University  
Ministry of Education Key Laboratory of Laser  
Life Science  
Guangzhou 510631 China  
and  
University of Colorado at Denver and  
Health Sciences Center  
Department of Radiation Oncology  
1665 North Ursula Street, F706  
Denver, Colorado 80202

**Abstract.** Singlet oxygen ( $^1\text{O}_2$ ) is an important factor mediating cell killing in photodynamic therapy (PDT). We previously reported that chemiluminescence (CL) can be used to detect  $^1\text{O}_2$  production in PDT and linked the signal to the PDT-induced cytotoxicity *in vitro*. We develop a new CL detection apparatus to achieve *in vivo* measurements. The system utilizes a time-delayed CL signal to overcome the interference from scattered excitation light, thus greatly improving the accuracy of the detection. The system is tested on healthy skin of BALB/ca mouse for its feasibility and reliability. The CL measurement is made during a synchronized gating period of the irradiation light. After each PDT treatment and *in situ* CL measurement, the skin response is scored over a period of 2 weeks. A remarkable relationship is observed between the score and the CL, regardless of the PDT treatment protocol. Although there are many issues yet to be addressed, our results clearly demonstrate the feasibility of CL measurement during PDT and its potential for *in vivo* PDT dosimetry. This requires further investigations. © 2008 Society of Photo-Optical Instrumentation Engineers. [DOI: 10.1117/1.2904961]

Keywords: photodynamic therapy; singlet oxygen; skin; chemiluminescence.

Paper 07122RR received Apr. 2, 2007; revised manuscript received Dec. 8, 2007; accepted for publication Dec. 11, 2007; published online Apr. 14, 2008.

## 1 Introduction

Photodynamic therapy (PDT) is a cell-killing process by light activation of a photosensitizer in the presence of oxygen.<sup>1-3</sup> It is well established that PDT cytotoxicity is mainly mediated via reactive oxygen species (ROS), i.e., singlet oxygen, produced during the light treatment.<sup>4-6</sup> Similar to other radiation therapies, proper dosimetry is required to warrant a successful PDT treatment. Given a particular tissue target with its intrinsic sensitivity to PDT, the effectiveness of a treatment depends on the interplay of three main factors: pharmacokinetics and biodistribution of the photosensitizer in the target, the light absorption by the photosensitizer molecules, and the availability of molecular oxygen.<sup>7</sup> Currently, clinical PDT dosimetry is still largely empirical and based on two descriptive parameters, delivered optical and drug “doses.”<sup>8</sup> The optical dose is often described as the energy fluence and fluence rate per unit area (for superficial irradiation) or per unit length (for interstitial irradiation). Although the optical inhomogeneity intrinsically associated with biological targets has been considered by researchers,<sup>9,10</sup> precise PDT dosimetry that links the treatment protocol directly to biological outcome remains a challenging task. The photosensitizer is typically prescribed based on patient body weight or body surface, regardless of the large intra- and interpatient variations in pharmacokinetic

ics. Recent developments in PDT dosimetry are achieved by either incorporating several of these parameters into a single metric<sup>9,11,12</sup> (e.g., photosensitizer bleaching, oxygen-conserving, etc.), or using certain biophysical/biological markers to predict PDT-induced tissue damage.<sup>13,14</sup> Clearly, given the complicated factors involved in PDT, a direct measurement of the cytotoxic agent produced during a treatment would provide superior dosimetry.<sup>15</sup>

It is generally accepted that  $^1\text{O}_2$  is one of the most important mediators for either direct cytotoxicity and/or cell death due to vascular damage caused by PDT. Monitoring the production of  $^1\text{O}_2$  by measuring its luminescence at 1270 nm would provide an ultimate marker and an ideal dosimetry technique.<sup>6,16</sup> Several issues limit the technique to be used as a routine means of PDT dosimetry.<sup>17</sup> The luminescence is extremely weak and is interfered with by not only the irradiation light, but also the autofluorescence. It requires a highly specialized and expensive photon multiplier tube (PMT) to acquire the luminescence signal that has a half-life-of the order of nanoseconds and at a 1270-nm wavelength. Although it has been shown, technically, it is possible to overcome these disadvantages; the complexity of the technical approach and the associated cost likely classify the technique as a gold standard of PDT dosimetry rather a routine method for practical applications.

Address all correspondence to Da Xing, MOE Key Laboratory of Laser Life Science, South China Normal University, Guangzhou 510631, China; Tel: 86-20-85210089; Fax: 86-20-85216052; E-mail: xingda@scnu.edu.cn

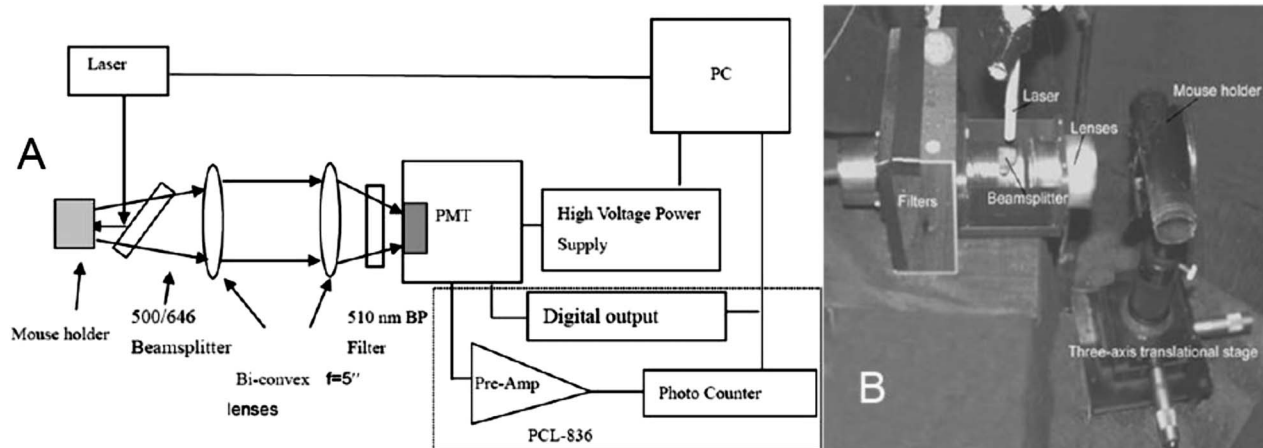


Fig. 1 Schematic of the experimental system for fluorescence measurements.

The objective of the study reported in this paper is to monitor  $^1\text{O}_2$  production using ROS-specific chemiluminescence (CL). Several CL probes<sup>18–20</sup> have been used to evaluate ROS production due to their high selectivity, sensitivity, and easy detection. ROS can chemically interact with probe molecules and transfer their potential energy to the latter. Upon that, the probe molecules, by changing their conformation, reach higher/excited energy state(s). During the subsequent deexcitation, photons in the visible wavelength range are emitted as CL. In general, CL is much stronger in signal strength and longer in lifetime, compared to that of the direct  $^1\text{O}_2$  luminescence, and thus can be easily detected by a conventional optical detection system such as<sup>21</sup> a PMT. With these good characteristics, much higher detection sensitivity and technical simplicity can be achieved.

In our experiment, we used a CL probe, fluoresceinyl cyridina luciferin analog [FCLA, [3, 7-Dihydro-6- [4-[2-[N'-(5-fluoresceinyl) thioureido] ethoxy] phenyl]-2-methylimidazo [1,2-a]pyrazin-3-one], that can selectively detect singlet oxygen and superoxide.<sup>22,23</sup> We previously reported that the FCLA CL is directly related to PDT cytotoxicity *in vitro*,<sup>24</sup> regardless of the treatment protocol. In this *in vivo* study, we detected  $^1\text{O}_2$  with the CL probe FCLA. We developed<sup>21</sup> a novel CL detection method by utilizing the decay character of CL to minimize the interference of the irradiation light. In this study, a novel CL measurement system aimed at *in vivo* applications was developed. By gating and synchronizing the irradiation light with the PMT system, we achieved an excellent SNR during *in vivo* measurements, practically eliminating the interference from the irradiation light. We further tested the method by comparing skin reactions with an array of PDT treatment protocols and the corresponding CL measured during the treatment. The results clearly demonstrate that *in vivo* CL measurement during PDT is feasible and there is a reliable correspondence between the CL and the biological outcome. Our study thus establishes an *in vivo* CL technique in PDT dosimetry as both effective and practical, and supports the need for further investigations.

## 2 Materials and Methods

### 2.1 Chemicals

For the ROS-specific CL probe, FCLA (Free Acid FCLA, Tokyo Kasei Kogyo Co., Tokyo, Japan) was dissolved in double-distilled water ( $100\ \mu\text{M}$ ) and stored at  $-80^\circ\text{C}$  until needed. The probe produces<sup>25</sup> a 532-nm CL and is at its maximum detection efficiency in the biological pH range. For the photosensitization reaction, photosensitizer protoporphyrin IX disodium salt (PpIX) (Aldrich Chemical Co., Milwaukee, Wisconsin) was prepared according to the manufacturer's directions to a concentration of  $200\ \mu\text{M}$ . The stock was stored in the dark at  $4^\circ\text{C}$  until needed.

### 2.2 Apparatus for Fluorescence and CL Detection

The schematic for fluorescence detection is shown in Fig. 1. For a semi-quantitative monitoring of the FCLA concentration in the target before PDT, FCLA fluorescence at 515 nm was monitored during the experiment.<sup>25</sup> The excitation light source was an argon-krypton laser (488 nm, Model 5500 ASL, Aiao Laser Co. Shanghai, China) and two filters [FF500/646-Di01-25  $\times$  36 to 45 deg beamsplitter, Semrock Co. USA, and a 510-nm bandpass (BP) filter, Oriol Co., USA.] were used to isolate the fluorescence signal from the irradiation light. The fluorescence was measured using a PMT (Model MP 952, PerkinElmer Optoelectronics, Wiesbaden, Germany) with a counter (PCL-836, Advantech Co., Ltd. Taiwan). The irradiation and fluorescence system is synchronized and controlled by LabVIEW (LabVIEW version 6.1 National Instruments, USA). For the *in vivo* experiment, a custom-built mouse holder was fixed on a three-axis translational stage and the position was optimized for maximizing the signal collection of the PMT [Fig. 1(B)].

The CL detection is similar to that for the fluorescence. The irradiation source for the photosensitization reaction is a custom-built, gated diode laser system (maximum power 100 mW, 635-nm laser diode controller, LDC 2000, ThorLab, and TEC 2000, Wavelength Electronics, USA). The laser system is controlled and modulated by the transistor-to-transistor

**Table 1** PDT treatment protocols.

Fluence Rate (mw/cm <sup>2</sup> )	Fluence (J/cm <sup>2</sup> )	PpIX ( $\mu$ mol)	Mice
10	40	0.02	6
30	40	0.02	6
30	30	0.02	6
30	20	0.02	6
30	10	0.02	6
50	40	0.02	6
0	0	0.02	6

logic (TTL) level of the counter. For the gated light irradiation and data acquisition, a 2-s irradiation was immediately followed by a 1-s data collection. A BP filter (530-nm BP filter, Oriel Co., USA) was used to protect the PMT from scattered irradiation light.

### 2.3 Experimental Protocols

BALB/ca mice of both genders (Center of Experimental Animal SunYat-sen University, Guangzhou, China) were used to provide an *in vivo* normal skin model. The mice were housed in an environmentally controlled animal facility with regular light/dark cycle. Before each experiment, the hind leg of a mouse was molted by depilatory (Na<sub>2</sub>S 8% aquasolution). For the *in vivo* PDT treatment and CL and fluorescence measurements, the mice were restrained using a custom-built holder without anesthesia. The animal holder was designed and fabricated to enable a hind leg to be positioned outside the holder without compromising its blood flow.

To simplify the experimental setup, in this pilot study, the pharmacokinetics of the FCLA were investigated in a separate experiment from the PDT-CL study. The 515-nm fluorescence of FCLA was continuously monitored in a separate animal after FCLA injection. The exposed mouse skin was irradiated with the argon-krypton laser, as already described, at 2  $\mu$ W/cm<sup>2</sup>. After collecting the control data (no drug injection), FCLA (0.01  $\mu$ mol) in 200- $\mu$ L physiologic saline was subcutaneously injected into the leg, and then the fluorescence signal collection was continued.

Premixed PpIX (0.02  $\mu$ mol) and FCLA (0.01  $\mu$ mol) in 200- $\mu$ L physiologic saline were injected subcutaneously into the leg, 1 h prior to the PDT light irradiation.<sup>26</sup> For PDT, each skin-exposed leg was irradiated with the 635-nm laser at a predetermined fluence and fluence rate (Table 1). The light irradiation was fractionated into 2 s/1 s light/dark cycle so CL signals could be collected during the dark periods. The mice were divided into six groups and treated accordingly ( $n=7$ /group, Table 1).

### 2.4 Method of Scoring PDT Effect

The normal skin response to PDT was evaluated in mice. A 1-cm-diam area of the hind limb was treated and then judged for the phototoxicity. A quantitative skin scoring system (Table

**Table 2** Skin response score for PDT treatment effect.

Score	Observation
0	No observable effect
1	Mild erythema
2	Moderate erythema
3	Strong erythema
4	Dry desquamation
5	Thin scab formation
6	Thick scab formation

2) was used to document photosensitivity by recording the appearance and decline of edema, erythema, and desquamation induced by each treatment.<sup>27</sup> The PDT treatment result, scored as the skin response, was recorded daily by a person who had no knowledge of the treatment protocol (single-blind method). A scoring system previously used on nude mice was adopted. With either nude or the regular mice used in this current study, the scoring system is only a pseudonumerical system based on objective observation of the skin response. These values give only an indication of the severity of the response, but not a true measurable degree of the biological outcome. The numerical values, thus, should not be compared directly among different animal models. To minimize the potential arbitrary associated with the objective scoring system, accumulated scores from each animal over a period of 2 weeks were used for evaluating the PDT response.

#### 2.4.1 Data analysis and statistics

Each PDT treatment protocol was repeated six times. Each animal was allowed to be treated only once. The results were analyzed accordingly. Parametric and nonparametric summary statistics are presented for each variable. Numerical data are presented as means  $\pm$  SE (standard error). Accumulated CL was calculated by integrating the CL signals over the measurement period.

## 3 Results

The temporal profile of FCLA fluorescence intensity during the FCLA injection and PDT procedure is shown in Fig. 2. When excited by light at 488 nm from an argon-ion laser, the probe (FCLA) has a strong fluorescence at its spectral peak value of 515 nm. In this study, monitoring of the FCLA diffusion and/or metabolism was performed *in situ*, but with a minor delay in signal collection to facilitate the drug infusion; thus, the interrupted continuity in the fluorescence temporal profile. After an initial surge due to the bolus injection, the FCLA fluorescence *in situ* increased steadily in the first hour until it reached a plateau, and remained steady thereafter for at least 1 h. The FCLA-CL measured immediately after pulsed laser irradiation is shown in Fig. 3. The CL signal shows a typical exponential decay character with an average half-life  $172 \pm 64$  ms (mean  $\pm$  SD). Figure 4 shows a repre-

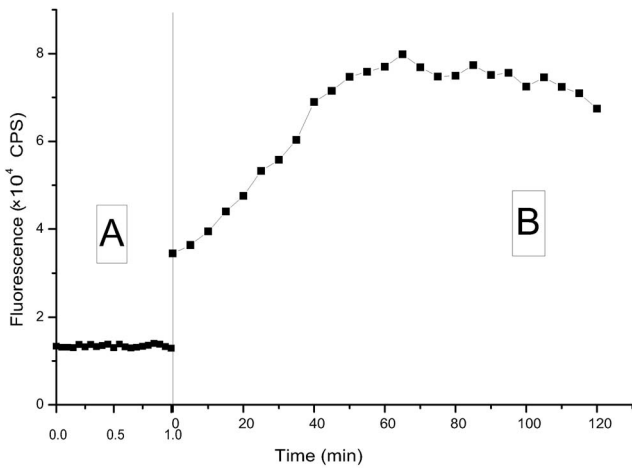


**Fig. 2** Temporal profile of FCLA fluorescence intensity measured *in situ* from normal mouse skin after local bolus injection (0.01  $\mu\text{mol}/200 \mu\text{L}$  saline): (A) background (without FCLA) and (B) the fluorescence signal immediately after the injection. CPS=counts per second.

sentative temporal profile of FCLA-CL intensity and its corresponding cumulative value during a PDT irradiation. The data indicate that while the irradiating fluence rates remained constant during a treatment, the corresponding CL intensity decreased over time.

Figure 5 shows the relationship between CL and various PDT treatment protocols from the *in vivo* mouse skin. The accumulated CL increases linearly with the total optical fluence [Fig. 5(A)]. As shown in Fig. 5(B), given identical total irradiation fluence, a higher irradiation fluence rate resulted in less CL, meaning, less  $^1\text{O}_2$ , compared to that produced with a lower irradiation fluence rate. After PDT treatment, the skin showed various degrees of response, depending on the treatment protocols. The maximum response occurred within 1

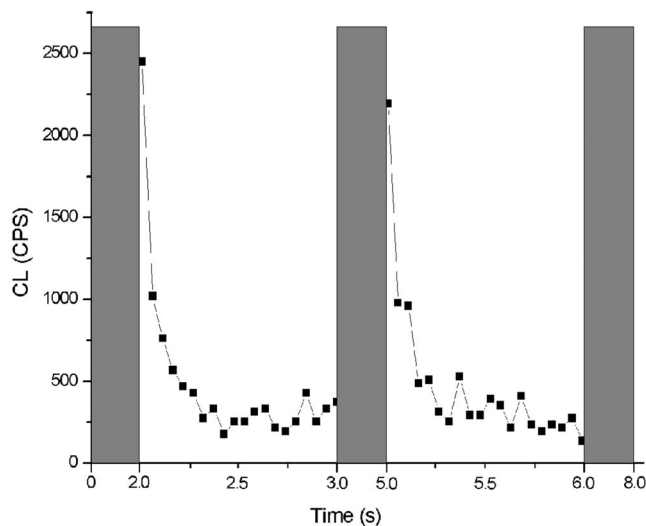


**Fig. 3** Real-time *in situ* CL measurement during interrupted PDT treatment. The X axis is not to scale and the gray columns indicate 2-s PDT irradiation periods.

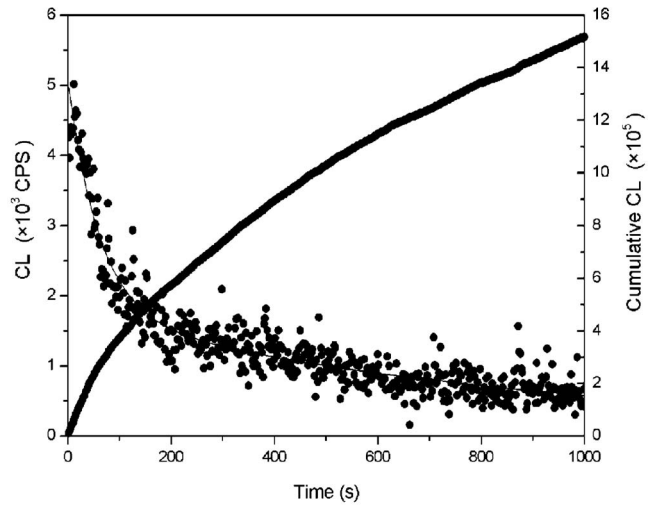


**Fig. 4** CL intensity ( $\bullet$ , left, Y axis) and cumulative CL (solid line, right Y axis) during PDT (x axis is irradiation time). The treatment protocol is fluence rate=30  $\text{mW}/\text{cm}^2$  and fluence=30  $\text{J}/\text{cm}^2$ .

week of the treatment and gradually recovered by the end of the 2-week follow-up period. At the same irradiation fluence rate, higher fluence produced more severe skin response [Fig. 6(A)]. With identical irradiation fluence, a higher irradiation fluence rate resulted in less prominent damage to the target [Fig. 6(B)]. The total skin response score, a sum of daily scores from each animal over the 2-week follow-up period, is shown in Fig. 7. Since the score, by definition, is not a true numerical evaluation of the skin response, we did not attempt linearity analysis of the data or statistical analysis for significant differences. Nevertheless, the graphs demonstrate that the skin response is dependent on both irradiation light fluence and fluence rate. On the other hand, a slight skin response with the 0- $\text{J}/\text{cm}^2$  dose can be seen in the graphs. The slight skin response without PDT treatment is likely due to the bolus injection itself.

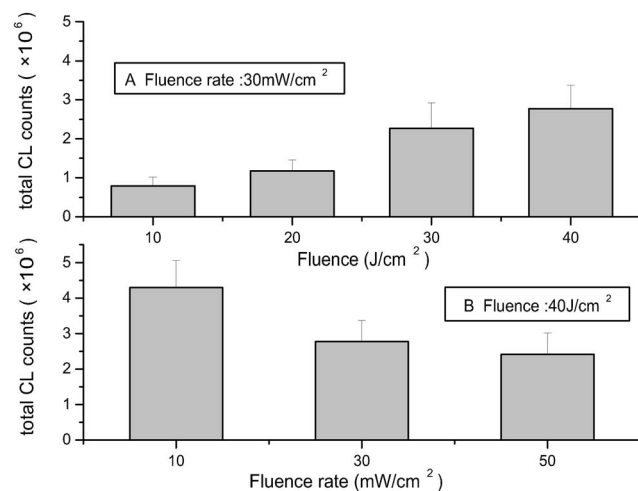


**Fig. 5** Relationships between accumulated CL and (A) irradiation fluence or (B) fluence rate.

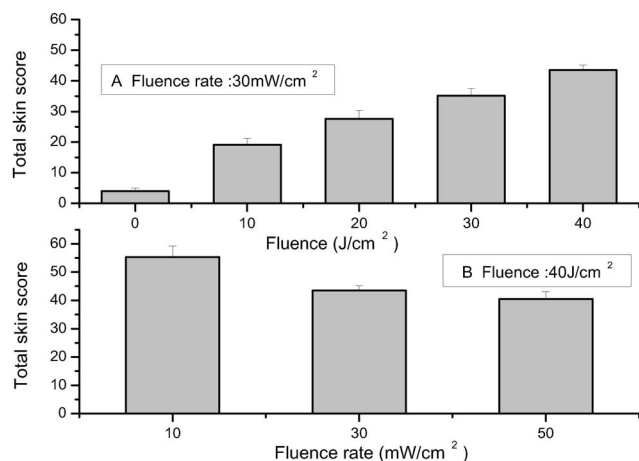


**Fig. 6** Relationships between skin response and (A) total fluence and (B) fluence rate.

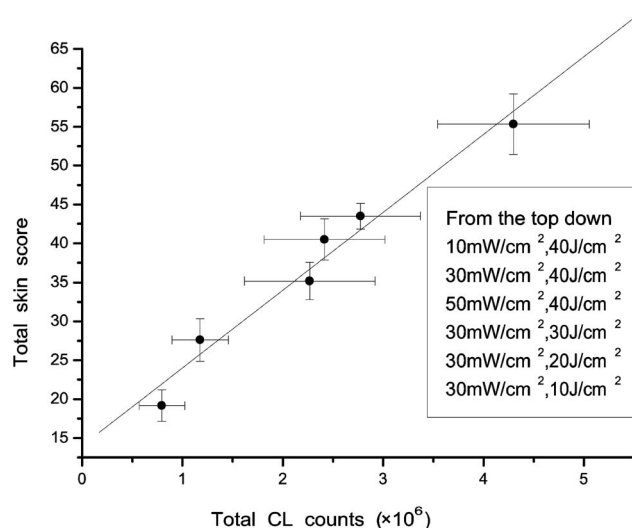


**Fig. 8** Relationship between accumulative CL and total skin scores without differentiating the treatment protocols. The linear fit is given as  $Y = 14 + 9.99 \times 10^{-6} X$  ( $R^2 = 0.97$ ).

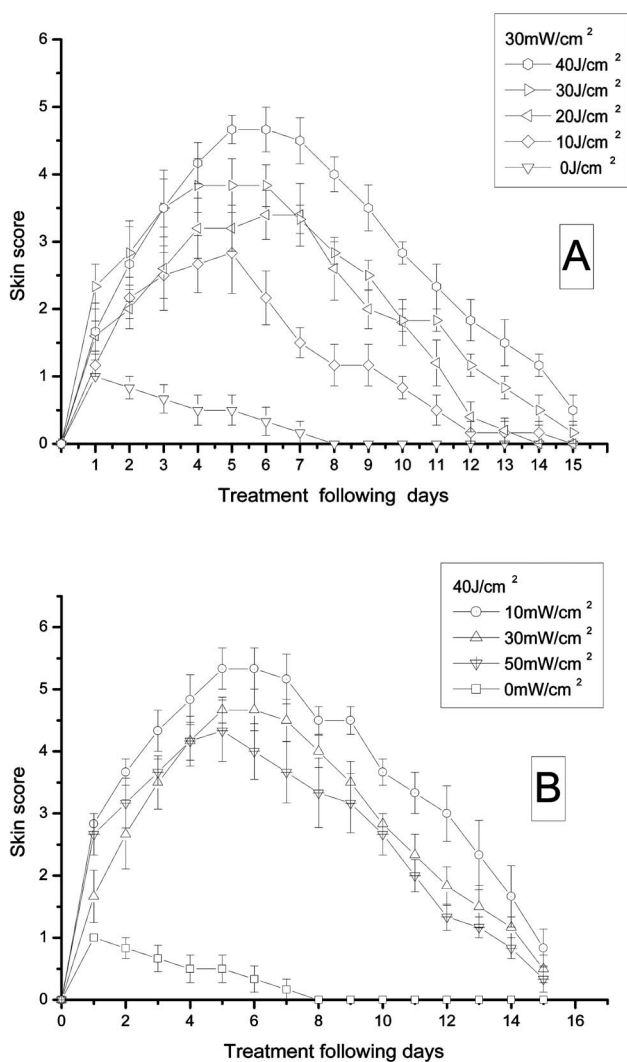


**Fig. 7** Skin score (mean  $\pm$  SE) after PDT by varying (A) total fluence or (B) fluence rate.

By pooling all accumulated CL and corresponding skin scores together, regardless of the treatment protocol, we obtained a chart showing the relationship between the production of the cytotoxic agent and its biological effects (Fig. 8). A linear regression fit was done in the figure ( $R^2 = 0.97$ ). Again, although linear regression may not have much true meaning due to the nature of the scoring system, the results clearly demonstrate that CL and the PDT biological effect has an excellent correspondence, with CL as a unique marker for predicting the biological effect.

#### 4 Discussion

On local injection, FCLA can either enter the systemic circulation or be temporarily taken up by cells. It has been demonstrated that FCLA can penetrate into the intracellular space rather efficiently.<sup>28</sup> By monitoring the FCLA fluorescence intensity over time, it is possible to study the local retention of FCLA. The data show that, after an initial 45-min increase, the skin retention of FCLA reaches a relatively stable phase lasting at least 1 h. This allows a reasonable time window for a CL measurement during a typical PDT treatment, without a significant effect due to the local FCLA concentration changes. Clearly, this conclusion applies only in the specific case of mouse skin. For other targets, more detailed studies must be conducted for potential changes in FCLA pharmacokinetics.

After completely cutting off the irradiating light, we measured the half-life of the FCLA CL to be approximately 200 ms. The autofluorescence of the skin has a much shorter lifetime and should have minimum impact on the result. This, consistent with that reported by others, shows that CL has a much longer life time than that of the <sup>1</sup>O<sub>2</sub> fluorescence.<sup>21,29</sup> The longer lifetime and an emission wavelength in the visible light range of CL translate into a more practical approach for <sup>1</sup>O<sub>2</sub> measurement, as it can be realized with conventional optical system such as those used in our study.

Note that the cumulative CL measured during PDT does not increase linearly with the irradiation time, due to a gradual decrease in the CL intensity (as shown by dots in Fig. 4). Considering that the local concentration of FCLA remains relatively stable during the course of the light irradiation, it is not likely that the pharmacokinetics of FCLA are a major factor contributing to be the CL decrease. The decrease in CL intensity over time is more likely due the following factors. It is well established that PDT can induce local oxygen depletion,<sup>30</sup> resulting in a decrease of  $^1\text{O}_2$  and, subsequently, a CL decrease. But the depletion would not affect the precision of detecting singlet oxygen with CL. Also the oxygen bleaching and supply may reach a dynamic equilibrium after a certain time, countered by local oxygen diffusion from local vasculature that is abundant in the skin. In addition, FCLA-CL is an irreversible chemical process. The CL probe is consumed during the process, causing CL decay, although its depletion is slow. These hypotheses require further investigation.

With PDT-induced changes of oxygen concentration, it is not surprising that given identical irradiation fluence, the total accumulated CL varies with the irradiation fluence rate. This is confirmed by the observation that higher irradiation fluence rate resulted less total CL production. Nevertheless, if the fluence rate is kept the same, statistically, the accumulated CL depends on the total light fluence increase.

The effect of PDT on skin took several days to maximize. This is a typical phenomenon of the treatment. With our current treatment protocol, the skin eventually recovered to normal or near normal condition, similar to that reported by others.<sup>31,32</sup> Since the skin response score is not a very objective evaluation and depends highly on the observer, we applied a concept of total skin response score by summing the scores from each animal over a fixed length of time. This was done to minimize the potential variations in individual scores. By comparing the total skin score to the treatment protocol, we found that the score increases as the total optical fluence increase, as expected. Given identical irradiation fluence, a higher fluence rate resulted in less total skin score/biological effect. Again, this coincides well with what has been well understood, that higher irradiation fluence rate causes more rapid oxygen and photosensitizer depletion,<sup>33</sup> thus less PDT efficiency.

The purpose of this study is to evaluate the feasibility of FCLA-CL as a PDT dosimetry marker. The choice of direct administration of exogenous PpIX instead of the usual ALA was due to the lower PDT efficiency of ALA in normal skin. Our preliminary investigation of ALA in the skin model yielded little CL signal, likely due to its lower concentration and subsequent generation of endogenous PpIX in the normal tissue, compared to that in tumor.

With the limited data collected in this study, it is premature to conclude that FCLA-CL can quantitatively predict the biological outcome of a PDT treatment. However, the data do indicate that accumulated CL is likely to reflect the total  $^1\text{O}_2$  production during a PDT treatment. It is well established that  $^1\text{O}_2$  is the main cytotoxic agent mediating PDT damage and there is strong evidence indicating the existence of a PDT damage threshold in various biological targets.<sup>34–36</sup> It is thus reasonable to conclude that the *in situ* CL measurement using

FCLA, a highly  $^1\text{O}_2$  selective probe, may provide an alternative marker for PDT dosimetry.

It is realized there are still many issues that must be addressed before the technique can be practically used in a PDT treatment. For example, for a practical tumor PDT treatment, the location(s) of CL signal collection and the optical system sensitivity required for *in vivo* monitoring still require further investigation. In the preliminary study, a 2 s/1 s light/dark cycle was used for PDT light irradiation and CL signal collection. The effect of such a “fractionated” PDT treatment has been studied by various investigators and the results, in general, suggest an improved biological effect due to improved tissue reoxygenation and other factors similarly observed in ionizing radiation therapy.<sup>37–40</sup> If the total treatment time is a concern, the dark period for CL collection can be decreased to the millisecond range, while multiple sampling will certainly improve the SNR ratio.

Although data from this study show that FCLA can remain in normal mouse skin for more than 1 h with little changes in its concentration, this may not be the case for other types of tissue. Colocalization of the photosensitizer and the CL probe must be considered for practical applications of the technique. A more detailed investigation of the interplay among the administration time of photosensitizer, CL probe, and light irradiation is critical to minimize the uncertainty caused by the difference in the pharmacokinetics of the drugs. Simultaneous monitoring of CL probe fluorescence during PDT treatment and CL measurement is a technically feasible approach, as shown in our preliminary study. With the technique, the local retention of the CL probe can be evaluated at real time and factored into the signal analysis.

Like any photons passing through a biological tissue, CL is inevitably subjected to the light scattering and absorption by the tissue before it is collected by an external optical detector, such as in this study. An interstitial isotropic optical fiber probe positioned at a designated location(s), i.e., distal tumor margin, for *in situ* CL collection is likely to minimize the uncertainty caused by light transmission in a tissue, at the same time, resolving the problem of limited CL diffusion range if it has to pass through layers of tissue to be detected.

### Acknowledgments

This research is supported by the National Natural Science Foundation of China (30470494; 30627003), the Natural Science Foundation of Guangdong Province (7117865), and the U.S. National Institutes of Health (NIH) Grant No. PO1-43892. Dr. Fred W. Hetzel of the University of Colorado Health Sciences Center (UCSCH), Colorado, provided invaluable scientific and editorial support to this manuscript.

### References

1. H. Kostron, A. Obwegeser, and R. Jakober, “Photodynamic therapy in neurosurgery: a review,” *J. Photochem. Photobiol.*, **B 36**, 157–168 (1996).
2. N. L. Oleinick, R. L. Morris, and I. Belichenko, “The role of apoptosis in response to photodynamic therapy: what, where, why, and how,” *Photochem. Photobiol. Sci.* **1**(1), 1–21 (2002).
3. S. B. Brown, E. A. Brown, and I. Walker, “The present and future role of photodynamic therapy in cancer treatment,” *Lancet Oncol.* **5**, 497–508 (2004).
4. C. S. Foote, “Definition of type I and type II photosensitized oxidation,” *Photochem. Photobiol.* **54**, 659–661 (1991).

5. J. Moan, Q. Peng, R. Sorensen, V. Iani, and J. M. Nesland, "The biophysical foundations of photodynamic therapy," *Endoscopy* **30**, 387–391 (1998).
6. J. Yamamoto, S. Yamamoto, T. Hirano, S. Y. Li, M. Koide, E. Kohno, M. Okada, C. Inenaga, T. Tokuyama, N. Yokota, S. Terakawa, and H. Namba, "Monitoring of singlet oxygen is useful for predicting the photodynamic effects in the treatment for experimental glioma," *Clin. Cancer Res.* **12**(23), 7132–7139 (2006).
7. D. Nowis, M. Makowski, T. Stokosa, M. Legat, T. Issat, and J. Golab "Direct tumor damage mechanisms of photodynamic therapy," *Acta Biochim. Pol.* **52**(2) 339–352 (2005).
8. G. M. Griffin, T. Zhu, M. Solonenko, F. D. Piero, A. Kapakin, T. M. Busch, A. Yodh, G. Polin, T. Bauer, D. Fraker, and S. M. Hahn1, "Preclinical evaluation of motexafin lutetium-mediated intraperitoneal photodynamic therapy in a canine model," *Clin. Cancer Res.* **7**(2), 374–381 (2001).
9. I. A. Boere, D. J. Robinson, H. S. de Bruijn, J. van den Boogert, H. W. Tilanus, H. J. Sterenborg, and R. W. de Bruin, "Monitoring in situ dosimetry and protoporphyrin IX fluorescence photobleaching in the normal rat esophagus during 5-aminolevulinic acid photodynamic therapy," *Photochem. Photobiol.* **78**(3), 271–278 (2003).
10. L. Lilge, N. Pomerleau-Dalcourt, A. Douplik, S. H. Selman, R. W. Keck, M. Szkudlarek, M. Pestka, and J. Jankun, "Transperineal in vivo fluence-rate dosimetry in the canine prostate during SnET2-mediated PDT," *Phys. Med. Biol.* **49**, 3209–3225 (2004).
11. M. C. G. Aalders, M. L. Triesscheijn, and M. Ruevekamp, "Doppler optical coherence tomography to monitor the effect of photodynamic therapy on tissue morphology and perfusion," *J. Biomed. Opt.* **11**, 044011 (2006).
12. B. W. Henderson, S. O. Gollnick, J. W. Snyder, T. M. Busch, P. C. Kousis, R. T. Cheney, and J. Morgan, "Choice of oxygen-conserving treatment regimen determines the inflammatory response and outcome of photodynamic therapy of tumors," *Cancer Res.* **64**(15), 2120–2126 (2004).
13. S. K. Bisland, J. W. Austin, D. P. Hubert, and L. Lilge, "Photodynamic actinometry using microspheres: concept, development and responsiveness," *Photochem. Photobiol.* **79**(4), 371–379 (2004).
14. S. B. Zhou, ZH. H. Zhang, Q. Liu, S. H. Q. Zeng, and Q. M. Luo, "The application of optical imaging: studying the photodynamic effect of tumor in vivo," *Prog. Biochem. Biophys.* **32**(10), 969–974 (2005).
15. B. C. Wilson, M. S. Patterson, and L. Lilge, "Implicit and explicit dosimetry in photodynamic therapy: a new paradigm," *Lasers Med. Sci.* **12**, 182–199 (1997).
16. M. J. Niedre, M. S. Patterson, and B. C. Wilson, "Direct near-infrared luminescence detection of singlet oxygen generated by photodynamic therapy in cells in vitro and tissues in vivo," *Photochem. Photobiol.* **75**, 382–391 (2002).
17. M. T. Jarvi, M. J. Niedre, M. S. Patterson, and B. C. Wilson, "Singlet oxygen luminescence dosimetry (SOLD) for photodynamic therapy: current status, challenges and future prospects," *Photochem. Photobiol.* **82**, 1198–1210 (2006).
18. X. H. Li, G. X. Zhang, H. M. Ma, D. Q. Zhang, J. Li, and D. B. Zhu, "4,5-dimethylthio-4'-[2-(9-anthryloxy)ethylthio]tetrathiafulvalene, a highly selective and sensitive chemiluminescence probe for singlet oxygen," *J. Am. Chem. Soc.* **126**, 11543–11548 (2004).
19. K. Teranishi and T. Nishiguchi, "Cyclodextrin-bound 6-(4-methoxyphenyl)imidazo[1,2-a]pyrazin-3(7H)-ones with fluorescein as green chemiluminescent probes for superoxide anions," *Anal. Biochem.* **325**, 185–195 (2004).
20. S. Sun, X. H. Li, G. X. Zhang, H. Ma, D. Q. Zhang, and Zh. J. Bao, "Determination of H<sub>2</sub>O<sub>2</sub>-dependent generation of singlet oxygen from human saliva with a novel chemiluminescence probe," *Biochim. Biophys. Acta* **1760**, 440–444 (2006).
21. Y. C. Wei, J. Zhou, D. Xing, and Q. Chen, "In vivo monitoring of singlet oxygen using delayed chemiluminescence during photodynamic therapy," *J. Biomed. Opt.* **12**(1), 014002 (2007).
22. M. Hao, D. Xing, Q. Chen, and J. Wang, "A high sensitivity detection method of singlet oxygen and superoxide anion," *Chin. Chem. Lett.* **15**(6), 679–682 (2004).
23. J. Wang, D. Xing, Y. H. He, and X. J. Hu, "Experimental study on photodynamic diagnosis of cancer mediated by chemiluminescence probe," *FEBS Lett.* **523**, 128–132 (2002).
24. Y. F. Qin, D. Xing, J. Zhou, S. M. Luo, and Q. Chen, "Feasibility of using fluoresceinyl cyridina luciferin analog in a novel chemiluminescence method for real-time photodynamic therapy dosimetry," *Photochem. Photobiol.* **81**(6), 1534–1538 (2005).
25. Y. h. He, D. Xing, S. C. Tan, Y. H. Tang, and K. I. Ueda, "In vivo sonoluminescence imaging with the assistance of FCLA," *Phys. Med. Biol.* **47**, 1535–1541 (2002).
26. I. Bronshtein, S. Aulova, A. Juzeniene, V. Iani, L. W. Ma, K. M. Smith, Z. Malik, J. Moan, and B. Ehrenberg, "In vitro and in vivo photosensitization by protoporphyrins possessing different lipophilicities and vertical localizaotion in the membrane," *Photochem. Photobiol.* **82**, 1319–1325 (2006).
27. D. J. Robinson, H. S. de Bruijn, N. van der Veen, M. R. Stringer, S. B. Brown, and W. M. Star, "Fluorescence photobleaching of ALA-induced protoporphyrin IX during photodynamic therapy of normal hairless mouse skin: the effect of light dose and irradiance and the resulting biological effect," *Photochem. Photobiol.* **67**, 140–149 (1998).
28. Y. X. Wu and D. Xing, "Permeating efficiency and localization of FCLA and HpD through membrane of lung, cancer cell," *Acta Laser Biol. Sin.* **14**(4), 287–291 (2005).
29. R. Schmidt, "The influence of heavy atoms on the deactivation of singlet oxygen ( $\delta$ ) in solution," *J. Am. Chem. Soc.* **111**, 6983–6987 (1989).
30. H. W. Wang, M. E. Putt, M. J. Emanuele, D. B. Shin, E. Glatstein, A. G. Yodh, and T. M. Busch, "Treatment-induced changes in tumor oxygenation predict photodynamic therapy outcome," *Cancer Res.* **64**, 7553–7561 (2004).
31. M. J. Niedre, C. S. Yu, M. S. Patterson, and B. C. Wilson, "Singlet oxygen luminescence as an in vivo photodynamic therapy dose metric: validation in normal mouse skin with topical amino-levulinic acid," *Br. J. Cancer* **92**, 298–304 (2005).
32. A. Ferrario, C. F. Chantrain, K. v. Tiehl, S. Buckley, N. Rucker, D. R. Shalinsky, H. Shimada, Y. A. Declerck, and C. J. Gomer, "The matrix metalloproteinase inhibitor prinomastat enhances photodynamic therapy responsiveness in a mouse tumor model," *Cancer Res.* **64**, 2328–2332 (2004).
33. S. Mitra and T. H. Foster, "Photochemical oxygen consumption sensitized by a porphyrin phosphorescent probe in two model systems," *Biophys. J.* **78**, 2597–2605 (2000).
34. Q. Chen, M. Chopp, L. Madigan, M. O. Dereski, and F. W. Hetzel, "Damage threshold of normal rat brain in photodynamic therapy," *Photochem. Photobiol.* **64**, 163–167 (1996).
35. B. W. Pogue, L. Lilge, M. S. Patterson, B. C. Wilson, and T. Hasan, "Absorbed photodynamic dose from pulsed versus continuous wave light examined with tissue-simulating dosimeters," *Appl. Opt.* **36**(28), 7257–7269 (1997).
36. T. J. Farrell, B. C. Wilson, M. S. Patterson, and M. C. Olivo, "Comparison of the in vivo photodynamic threshold dose for photofrin mono- and tetrasulfonated aluminum phthalocyanine using a rat liver model," *Photochem. Photobiol.* **68**, 394–399 (1998).
37. S. K. Bisland, L. Lilge, A. Lin, R. Rusnov, and B. C. Wilson, "Metronomic photodynamic therapy as a new paradigm for photodynamic therapy: rationale and preclinical evaluation of technical feasibility for treating malignant brain tumors," *Photochem. Photobiol.* **80**, 22–30 (2004).
38. A. Bogaards, A. Varma, K. Zhang, D. Zach, L. Lilge, P. J. Muller, and B. C. Wilson, "Fluorescence image-guided brain tumour resection with adjuvant metronomic photodynamic therapy: pre-clinical model and technology development," *Photochem. Photobiol. Sci.* **4**(5), 438–442 (2005).
39. P. S. Thong, F. Watt, M. Q. Ren, P. H. Tan, K. C. Soo, and M. Olivo, "Hypericin-photodynamic therapy (PDT) using an alternative treatment regime suitable for multi-fraction PDT," *J. Photochem. Photobiol., B* **82**(1), 1–8 (2006).
40. L. Harrison and K. Blackwell, "Hypoxia and anemia: factors in decreased sensitivity to radiation therapy and chemotherapy?," *Oncologist* **9**(5), 31–40 (2004).